

Modeling Crop Photosynthesis— from Biochemistry to Canopy

Proceedings of a symposium sponsored by Division C-2 of the Crop Science Society of America and Division A-3 of the American Society of Agronomy in Anaheim, California, 29 Nov. 1988.

Editors

K. J. Boote and R. S. Loomis

Organizing Committee

K. J. Boote

Editor-in-Chief CSSA

C. W. Stuber

Editor-in-Chief ASA

G. A. Peterson

Managing Editor

S. H. Mickelson

Assistant Editor

P. Kasper

CSSA Special Publication Number 19

**Crop Science Society of America, Inc.
American Society of Agronomy, Inc.
Madison, Wisconsin, USA
1991**

Copyright © 1991 by the Crop Science Society of America, Inc.
American Society of Agronomy, Inc.

ALL RIGHTS RESERVED UNDER THE U.S. COPYRIGHT
LAW OF 1978 (P.L. 94-533)

Any and all uses beyond the limitations of the "fair use" provision
of the law require written permission from the publisher(s) and/or
the author(s); not applicable to contributions prepared by officers or
employees of the U.S. Government as part of their official duties.

Crop Science Society of America, Inc.
American Society of Agronomy, Inc.
677 South Segoe Road, Madison, WI 53711, USA

Second Printing 1992

Library of Congress Cataloging-in-Publication Data

Modeling crop photosynthesis—from biochemistry to canopy : proceed-
ings of a symposium / sponsored by Division C-2 of the Crop Science
Society of America and Division A-3 of the American Society of
Agronomy in Anaheim, California, 29 Nov. 1988 ; editors, K.J. Boote
and R.S. Loomis.

p. cm. — (CSSA special publication : no. 19)

Includes bibliographical references.

ISBN 0-89118-533-X

1. Photosynthesis—Computer simulation—Congresses.

2. Crops—Physiology—Computer simulation—Congresses.

I. Boote, K.J. II. Loomis, R.S. III. Crop Science Society of Ameri-
ca. Division C-2. IV. American Society of Agronomy. Division A-3.
V. Series.

QK882.M8 1991

581.1'3342—dc20

91-26613

CIP

Printed in the United States of America

Modeling Crop Photosynthesis— from Biochemistry to Canopy

FOREWORD

Photosynthesis is the most important biochemical process in nature. The rates at which plants fix CO_2 , under the wide range of conditions found in nature, determine their productivity and ultimate utility to humans. As scientists have learned more about factors that limit and control this complex process, new genetic and management strategies have been devised to more fully exploit and develop its potential.

The models described in the chapters in this volume summarize the state of knowledge regarding the interactions of environmental and biochemical factors on crop photosynthesis. These models are not only valuable research tools but, when integrated into sophisticated crop simulation models, they become powerful tools to improve the management of crop production systems. Crop producers must strive to address environmental concerns and remain economically competitive. Computer models can be immensely valuable aids.

Crop simulation models need to accurately reflect actual biological happenings under complex and rapidly changing conditions. Such models must be based on accurate and reliable information regarding the most fundamental of plant processes — photosynthesis. The authors of this volume have made significant strides toward this end. Their work is to be commended.

V. L. LECHTENBERG, *president*
Crop Science Society of America

D. R. NIELSEN, *president*
American Society of Agronomy

PREFACE

Explanation and prediction of the growth of managed and natural ecosystems in response to climatic and soil-related factors are increasingly important as objectives of our science. Quantitative prediction of complex systems, however, depends on integrating information through levels of organization, and the principal approach we have for that is through the construction of simulation models. Simulation of the system's use and balance of C, beginning with the input of C from canopy assimilation, forms the essential core of most simulation models that deal with the growth of vegetation.

It is now more than 40 yr since the first detailed model of canopy light interception was reported by Monsi and Saeki (1948). That work was followed by more advanced geometrical and physiological models of foliage canopies by de Wit (1965), the Estonian group (summarized by Ross, 1981), and Duncan et al. (1967). The sophistication of the models for canopy light interception was not matched in the area of models for biochemistry-physiology of photosynthesis until the past 10 yr, when the Glasshouse Crops Group in England (Acock, Ch. 3 in this book) and Farquhar and von Caemmerer (1982) began to publish advanced approaches to that problem.

Parallel progress was made in the development of dynamic simulation models of the growth of crops. Crop model development was stimulated by Forrester's (1961) state-variable approach to system simulation and by access to mainframe computers and, more recently, powerful microcomputers. Of necessity, early crop models employed simple, summary approaches to the simulation of photosynthesis. Presently, simulation studies are no longer limited by one's mainframe budgets, and quite complicated models are processed quickly on microcomputers. It is now appropriate to determine whether more sophisticated approaches for light interception, photosynthetic biochemistry, and canopy photosynthesis can be incorporated into crop models, and to determine the utility of adding such sophisticated approaches in contrast to refining summary approaches.

In this publication, the contributing authors have summarized some of the approaches now used to predict leaf and canopy photosynthesis. Most of these models can stand alone for studies of photosynthesis, or they can be incorporated into crop growth models. Models for single-leaf response to light, CO_2 , and temperature are succinctly described in the first two chapters (Evans and Farquhar, Ch. 1; Harley and Tenhunen, Ch. 2). Norman and Arkebauer (Ch. 5) and Gutschick (Ch. 4) illustrate how numerical, layered-canopy, simulation models describing complete radiation, energy, water vapor, and CO_2 balances among leaf strata can be used to predict whole-canopy assimilation response to light, CO_2 , wind speed, humidity, and temperature. Gutschick shows how it is possible to reduce a complex numerical model into a summary model that provides important insights for agricultural production and water-use efficiency. Acock (Ch. 3) introduces alternative approaches for predicting whole-canopy response to light, CO_2 ,

and temperature. Sinclair's chapter (Ch. 6) contributes an important advance in simple canopy models, particularly incorporation of the effects of leaf N content on canopy assimilation. Lastly, Boote and Loomis (Ch. 7) review the approaches taken by the various authors to describe leaf and canopy assimilation processes, and then present simplified equations for predicting canopy assimilation response to light, leaf area index, and incomplete hedge-row canopy coverage.

REFERENCES

- de Wit, C.T. 1965. Photosynthesis of leaf canopies. Agric. Res. Rep. no. 663. PUDOC, Wageningen, the Netherlands.
- Duncan, W.G., R.S. Loomis, W.A. Williams, and R. Hanau. 1967. A model for simulating photosynthesis in plant communities. *Hilgardia* 38:181-205.
- Farquhar, G.D., and S. von Caemmerer. 1982. Modeling of photosynthetic response to environment. p. 549-587. *In* O.L. Lang et al. (ed.) *Physiological plant ecology II*. New Ser. Vol. 12B. Encyclopedia of plant physiology. Springer-Verlag, Berlin.
- Forrester, J.W. 1961. *Industrial dynamics*. Massachusetts Inst. Technol. Press, Cambridge, MA.
- Monsi, M., and T. Saeki. 1953. Über den Lichhfaktor in den Pflangengesellschaften und seine Bedeutung für die Stoffproduktion. *Jpn. J. Bot.* 14:22-52.
- Ross, J. 1981. The radiation regime and architecture of plant stands. *Tasks for vegetative sciences* no. 3. Junk, The Hague.

K.J. BOOTE and R.S. LOOMIS
Editors

CONTRIBUTORS

Basil Acock	Research Leader, USDA-ARS, NRI, Systems Research Laboratory, BARC-West, Beltsville, MD 20705-2350
T. J. Arkebauer	Assistant Professor, Department of Agronomy, University of Nebraska, Lincoln, NE 68583-0817
K. J. Boote	Professor of Agronomy, Agronomy Department, University of Florida, Gainesville, FL 32611
John R. Evans	Professor, P.E.B. Research School of Biological Sciences, Australian National University, Canberra 2601, Australia
Graham D. Farquhar	Professor, P.E.B. Research School of Biological Sciences, Australian National University, Canberra 2601, Australia
Vincent P. Gutschick	Professor of Biology, Department of Biology, New Mexico State University, Las Cruces, NM 88003
Peter C. Harley	Research Scientist, Systems Ecology Research Group, San Diego State University, San Diego, CA 92182
R. S. Loomis	Professor of Agronomy, Department of Agronomy and Range Science, University of California, Davis, CA 95616
J. M. Norman	Professor of Soil Science, Department of Soil Science, University of Wisconsin, Madison, WI 53706
Thomas R. Sinclair	Plant Physiologist, USDA-ARS, Agronomy-Physiology Laboratory, University of Florida, Gainesville, FL 32611
J. D. Tenhunen	Associate Director, Systems Ecology Research Group, San Diego State University, San Diego, CA 92182

Conversion Factors for SI and non-SI Units

Conversion Factors for SI and non-SI Units

To convert Column 1 into Column 2, multiply by	Column 1 SI Unit	Column 2 non-SI Unit	To convert Column 2 into Column 1, multiply by
Length			
0.621	kilometer, km (10 ³ m)	mile, mi	1.609
1.094	meter, m	yard, yd	0.914
3.28	meter, m	foot, ft	0.304
1.0	micrometer, μm (10 ⁻⁶ m)	micron, μ	1.0
3.94 × 10 ⁻²	millimeter, mm (10 ⁻³ m)	inch, in	25.4
10	nanometer, nm (10 ⁻⁹ m)	Angstrom, Å	0.1
Area			
2.47	hectare, ha	acre	0.405
247	square kilometer, km ² (10 ³ m) ²	acre	4.05 × 10 ⁻³
0.386	square kilometer, km ² (10 ³ m) ²	square mile, mi ²	2.590
2.47 × 10 ⁻⁴	square meter, m ²	acre	4.05 × 10 ³
10.76	square meter, m ²	square foot, ft ²	9.29 × 10 ⁻²
1.55 × 10 ⁻³	square millimeter, mm ² (10 ⁻³ m) ²	square inch, in ²	645
Volume			
9.73 × 10 ⁻³	cubic meter, m ³	acre-inch	102.8
35.3	cubic meter, m ³	cubic foot, ft ³	2.83 × 10 ⁻²
6.10 × 10 ⁴	cubic meter, m ³	cubic inch, in ³	1.64 × 10 ⁻⁵
2.84 × 10 ⁻²	liter, L (10 ⁻³ m ³)	bushel, bu	35.24
1.057	liter, L (10 ⁻³ m ³)	quart (liquid), qt	0.946
3.53 × 10 ⁻²	liter, L (10 ⁻³ m ³)	cubic foot, ft ³	28.3
0.265	liter, L (10 ⁻³ m ³)	gallon	3.78
33.78	liter, L (10 ⁻³ m ³)	ounce (fluid), oz	2.96 × 10 ⁻²
2.11	liter, L (10 ⁻³ m ³)	pint (fluid), pt	0.473

Mass

2.20×10^{-3}	gram, g (10^{-3} kg)	pound, lb	454
3.52×10^{-2}	gram, g (10^{-3} kg)	ounce (avdp), oz	28.4
2.205	kilogram, kg	pound, lb	0.454
0.01	kilogram, kg	quintal (metric), q	100
1.10×10^{-3}	kilogram, kg	ton (2000 lb), ton	907
1.102	megagram, Mg (tonne)	ton (U.S.), ton	0.907
1.102	tonne, t	ton (U.S.), ton	0.907

Yield and Rate

0.893	kilogram per hectare, kg ha ⁻¹	pound per acre, lb acre ⁻¹	1.12
7.77×10^{-2}	kilogram per cubic meter, kg m ⁻³	pound per bushel, bu ⁻¹	12.87
1.49×10^{-2}	kilogram per hectare, kg ha ⁻¹	bushel per acre, 60 lb	67.19
1.59×10^{-2}	kilogram per hectare, kg ha ⁻¹	bushel per acre, 56 lb	62.71
1.86×10^{-2}	kilogram per hectare, kg ha ⁻¹	bushel per acre, 48 lb	53.75
0.107	liter per hectare, L ha ⁻¹	gallon per acre	9.35
893	tonnes per hectare, t ha ⁻¹	pound per acre, lb acre ⁻¹	1.12×10^{-3}
893	megagram per hectare, Mg ha ⁻¹	pound per acre, lb acre ⁻¹	1.12×10^{-3}
0.446	megagram per hectare, Mg ha ⁻¹	ton (2000 lb) per acre, ton acre ⁻¹	2.24
2.24	meter per second, m s ⁻¹	mile per hour	0.447

Specific Surface

10	square meter per kilogram, m ² kg ⁻¹	square centimeter per gram, cm ² g ⁻¹	0.1
1000	square meter per kilogram, m ² kg ⁻¹	square millimeter per gram, mm ² g ⁻¹	0.001

Pressure

9.90	megapascal, MPa (10^6 Pa)	atmosphere	0.101
10	megapascal, MPa (10^6 Pa)	bar	0.1
1.00	megagram per cubic meter, Mg m ⁻³	gram per cubic centimeter, g cm ⁻³	1.00
2.09×10^{-2}	pascal, Pa	pound per square foot, lb ft ⁻²	47.9
1.45×10^{-4}	pascal, Pa	pound per square inch, lb in ⁻²	6.90×10^3

(continued on next page)

Conversion Factors for SI and non-SI Units

To convert Column 1 into Column 2, multiply by		Column 1 SI Unit	Column 2 non-SI Unit	To convert Column 2 into Column 1, multiply by
Temperature				
1.00 (K - 273) (9/5 °C) + 32		Kelvin, K Celsius, °C	Celsius, °C Fahrenheit, °F	1.00 (°C + 273) 5/9 (°F - 32)
Energy, Work, Quantity of Heat				
9.52 × 10 ⁻⁴ 0.239 10 ⁷ 0.735 2.387 × 10 ⁻⁵ 10 ⁵ 1.43 × 10 ⁻³		joule, J joule, J joule, J joule, J joule per square meter, J m ⁻² newton, N watt per square meter, W m ⁻²	British thermal unit, Btu calorie, cal erg foot-pound calorie per square centimeter (langley) dyne calorie per square centimeter minute (irradiance), cal cm ⁻² min ⁻¹	1.05 × 10 ³ 4.19 10 ⁻⁷ 1.36 4.19 × 10 ⁴ 10 ⁻⁵ 698
Transpiration and Photosynthesis				
3.60 × 10 ⁻² 5.56 × 10 ⁻³ 10 ⁻⁴ 35.97		milligram per square meter second, mg m ⁻² s ⁻¹ milligram (H ₂ O) per square meter second, mg m ⁻² s ⁻¹ milligram per square meter second, mg m ⁻² s ⁻¹ milligram per square meter second, mg m ⁻² s ⁻¹	gram per square decimeter hour, g dm ⁻² h ⁻¹ micromole (H ₂ O) per square centimeter second, μmol cm ⁻² s ⁻¹ milligram per square centimeter second, mg cm ⁻² s ⁻¹ milligram per square decimeter hour, mg dm ⁻² h ⁻¹	27.8 180 10 ⁴ 2.78 × 10 ⁻²
Plane Angle				
57.3		radian, rad	degrees (angle), °	1.75 × 10 ⁻²

Electrical Conductivity, Electricity, and Magnetism

10	siemen per meter, $S\ m^{-1}$	millimho per centimeter, mmho cm^{-1}	0.1
10^4	tesla, T	gauss, G	10^{-4}

Water Measurement

9.73×10^{-3}	cubic meter, m^3	acre-inches, acre-in	102.8
9.81×10^{-3}	cubic meter per hour, $m^3\ h^{-1}$	cubic feet per second, $ft^3\ s^{-1}$	101.9
4.40	cubic meter per hour, $m^3\ h^{-1}$	U.S. gallons per minute, gal min^{-1}	0.227
8.11	hectare-meters, ha-m	acre-feet, acre-ft	0.123
97.28	hectare-meters, ha-m	acre-inches, acre-in	1.03×10^{-2}
8.1×10^{-2}	hectare-centimeters, ha-cm	acre-feet, acre-ft	12.33

Concentrations

1	centimole per kilogram, $cmol\ kg^{-1}$ (ion exchange capacity)	milliequivalents per 100 grams, meq $100\ g^{-1}$	1
0.1	gram per kilogram, $g\ kg^{-1}$	percent, %	10
1	milligram per kilogram, $mg\ kg^{-1}$	parts per million, ppm	1

Radioactivity

2.7×10^{-11}	becquerel, Bq	curie, Ci	3.7×10^{10}
2.7×10^{-2}	becquerel per kilogram, $Bq\ kg^{-1}$	picrocurie per gram, pCi g^{-1}	37
100	gray, Gy (absorbed dose)	rad, rd	0.01
100	sievert, Sv (equivalent dose)	rem (roentgen equivalent man)	0.01

Plant Nutrient Conversion

<i>Elemental</i>		<i>Oxide</i>	
2.29	P	P_2O_5	0.437
1.20	K	K_2O	0.830
1.39	Ca	CaO	0.715
1.66	Mg	MgO	0.602

CONTENTS

Foreword	vii
Preface	ix
Contributors	xi
Conversion Factors for SI and non-SI Units	xiii
1 Modeling Canopy Photosynthesis from the Biochemistry of the C ₃ Chloroplast John R. Evans and Graham D. Farquhar	1
2 Modeling the Photosynthetic Response of C ₃ Leaves to Environmental Factors P. C. Harley and J. D. Tenhunen	17
3 Modeling Canopy Photosynthetic Response to Carbon Dioxide, Light Interception, Temperature, and Leaf Traits Basil Acock	41
4 Modeling Photosynthesis and Water-Use Efficiency of Canopies as Affected by Leaf and Canopy Traits Vincent P. Gutschick	57
5 Predicting Canopy Photosynthesis and Light-Use Efficiency from Leaf Characteristics J. M. Norman and T. J. Arkebauer	75
6 Canopy Carbon Assimilation and Crop Radiation-Use Efficiency Dependence on Leaf Nitrogen Content T. R. Sinclair	95
7 The Prediction of Canopy Assimilation K. J. Boote and R. S. Loomis	109

Modeling Canopy Photosynthesis from the Biochemistry of the C_3 Chloroplast

John R. Evans and Graham D. Farquhar

*Australian National University
Canberra, Australia*

Photosynthesis involves the interception of light energy and its conversion to chemical energy in intermediates of high chemical potential, which are then used to drive the catalytic fixation of CO_2 into sugars and other compounds. Hundreds of different proteins are involved along the way but, despite this complexity, there are several key factors that allow simplification in our model of the system. Attention can be focused on the principal CO_2 -fixing enzyme ribulose-1,5-bisphosphate (RuBP) carboxylase-oxygenase, Rubisco, which is the most abundant leaf protein. To achieve adequate rates of CO_2 assimilation, Rubisco need to be abundant because it has a low affinity for CO_2 and a relatively slow rate of catalysis. Rubisco also catalyzes the competitive reaction between RuBP and O_2 and considerable metabolic effort by the cell is required to recover the C skeleton in phosphoglycolate that is so produced. The kinetics of the Rubisco enzyme, with respect to its substrates RuBP, CO_2 and O_2 encompass a large proportion of the photosynthetic properties of a leaf. We will present the basic equations that have been discussed in detail elsewhere (Farquhar & von Caemmerer, 1982), with particular emphasis on how they apply to canopy photosynthesis. Since the publication of the model by Farquhar et al. (1980), considerable experimental evidence has been obtained that substantiates much of the theory and has enriched the detail of the underlying biochemical mechanisms of the model.

In order to gain CO_2 , the leaf loses water to the atmosphere. The amount of water lost per C gained depends, firstly, on the water vapor-pressure difference between the leaf and the air. Second, it depends on the intercellular partial pressure of CO_2 , pCO_2 . Conventional methods of assessing the transpiration-use efficiency, W (amount of C gained per water used), involve careful measurements of soil moisture by either weighing pots or using neutron probes. This has proved rather impractical on the scale necessary for plant breeding programs. A new technique that involves the determination of the $^{13}C/^{12}C$ ratio of the plant can be used to assess the

integrated value of intercellular $p\text{CO}_2$ and this enables transpiration-use efficiency to become a selection criterion. The underlying theory (Farquhar et al., 1982) is currently being evaluated in the context of plant breeding with several crops (e.g., wheat [*Triticum aestivum* L.], Farquhar & Richards, 1984; Condon et al., 1987; and peanut [*Arachis hypogaea* L.], Hubick et al., 1986. See also Farquhar et al., 1988). The basic equations will be presented here because this technique offers an exciting new avenue for plant improvement where yield is limited by the availability of water.

RATE OF CARBON DIOXIDE ASSIMILATION

The absorption of light by the pigments in the chloroplast membranes leads to the transfer of electrons from H_2O to nicotinamide adenine dinucleotide phosphate (NADP^+) to make NADPH, and the buildup of protons in the lumen of the thylakoids. The protons drive the regeneration of the high-energy compound adenosine triphosphate (ATP), catalyzed by the coupling factor. These two high-potential intermediates, NADPH and ATP, are used in the reactions of the C-reduction cycle to regenerate the substrate for CO_2 fixation, RuBP. Because of the high concentration of Rubisco in the chloroplast, the kinetics of the enzyme with respect to its substrate RuBP do not follow normal Michaelis-Menten kinetics (Farquhar, 1979). Rather, we think of Rubisco as either being limited by RuBP or not. The pool size of RuBP is small, and without continuous regeneration would be consumed within seconds. Since RuBP regeneration is closely coupled to the rate of electron transport and photophosphorylation, the RuBP-limited Rubisco velocity closely reflects the rate of electron transport. When RuBP is saturating, the photosynthetic properties reflect the affinity of Rubisco for CO_2 and the relative rates of oxygenation and carboxylation. The potential rate of electron transport declines at lower temperatures to a greater extent than does Rubisco activity; thus, the balance between the two capacities changes with temperature. In some low-temperature situations, phosphate recycling to the chloroplast prevents the potential rate of electron transport from being reached (Sharkey, 1985; Sage & Sharkey, 1987; Labate & Leegood, 1988). We will focus on the electron-transport properties, because the photosynthetic rate of many crop canopies is primarily light limited.

IRRADIANCE RESPONSE CURVES

The many steps between light absorption and RuBP regeneration, in combination with the complexity of the optics of the leaf, mean that a precise theoretical justification for Eq. [1] is not possible at present. However, the following equation can describe very precisely the relationship between potential electron transport rate, J , and the irradiance usefully absorbed by Photosystem II, I_2 :

$$\Theta J^2 - (I_2 + J_{\max})J + I_2 J_{\max} = 0 \quad [1]$$

which can be solved for J as follows:

$$J = \{I_2 + J_{\max} - [(I_2 + J_{\max})^2 - 4\Theta I_2 J_{\max}]^{1/2}\} / 2\Theta \quad [2]$$

where I_2 is related to the incident irradiance (400–700 nm), I_0 , as follows: $I_2 = I_0 (1 - f)(1 - r)/2$. The factor f corrects for the spectral imbalance of the light (~ 0.15 , see Evans, 1987a), r is the reflectance plus any small transmittance of the leaf or crop to photosynthetically active radiation (~ 0.12); I_0 is divided by 2 because light is absorbed by both Photosystem II and Photosystem I to drive one electron from H_2O to NADP^+ . The maximum rate of electron transport, J_{\max} , is a property of the thylakoids that varies depending on growth conditions. The factor Θ is a curvature factor, $0 \leq \Theta \leq 1$, which determines how quickly the transition is made from the region of maximum quantum yield to the light-saturated rate. When $\Theta = 0$, the equation degenerates to a rectangular hyperbola, while $\Theta = 1$ describes the Blackman response of two straight lines representing light-dependent and light-saturated rates.

The region of maximum quantum yield is found at low irradiance, where the rate of photosynthesis is linearly related to the irradiance. No significant variation is seen across a broad range of C_3 plants in the quantum yield measured as O_2 evolution in saturating CO_2 , when expressed on an absorbed-light basis (Björkman & Demmig, 1987; Evans, 1987a). The absolute value of the quantum yield depends on the wavelength or spectral composition of the light (McCree, 1972; Inada, 1976). For sunlight, the quantum yield is about 15% below the maximum, which occurs with 600-nm light (Evans, 1987a). To correct for this, the incident irradiance is multiplied by the term $(1 - f)$.

The light-saturated rate of electron transport per unit leaf area is determined primarily by two factors. First, the capacity scales in proportion with the chlorophyll content per unit leaf area (Fig. 1-1A). This reflects the amount of photosynthetic apparatus in a given leaf area. Leaves that develop with a restricted N supply contain less N per unit leaf area. This corresponds to smaller protein contents in all fractions of the leaf. A similar situation can be reached during senescence, where N is progressively remobilized from the leaf.

The second determinant of the electron-transport capacity relates to the irradiance during growth of the leaf. The electron-transport capacity per unit of chlorophyll is less in leaves acclimated to low irradiance (Fig. 1-1B). This reflects the altered composition of the thylakoid membranes. When acclimated to low irradiance, thylakoid membranes are enriched in the light-harvesting chlorophyll a/b protein complex and depleted in Photosystem II reaction-center complexes, plastoquinone, cytochrome b/f complexes, coupling factor, and ferredoxin NADP reductase (Anderson, 1986). The electron-transport capacity increases as the relative abundance of plastoquinone, cytochrome f, coupling factor, and ferredoxin NADP reductase increases (Evans, 1987b; Terashima & Evans, 1988). The value of J_{\max} correlates strongly with the cytochrome f content of the leaf (Terashima &

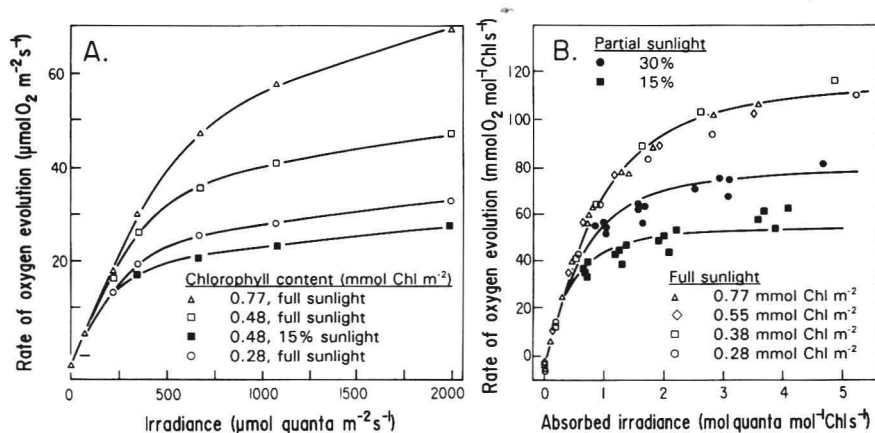


Fig. 1-1. Irradiance response curves of spinach leaves measured in a leaf-disk, O_2 electrode (Delieu & Walker, 1981) at 25°C and 1% CO_2 , expressed on the basis of (A) leaf area or (B) chlorophyll content. Plants were grown under full ($\approx 2 \text{ mmol quanta m}^{-2} \text{ s}^{-1}$) or partial sunlight with different NO_3^- nutrition, which caused the leaf chlorophyll content to vary. Lines were calculated using Eq. [2], with $J_{\text{max}} = 500, 210$, and $143 \text{ mmol e}^- (\text{mol Chl})^{-1} \text{ s}^{-1}$ for the 100, 30, and 15% irradiance treatments, respectively, $\Theta = 0.69$ and $f = 0.15$. (Data from Evans & Terashima, 1987; Terashima & Evans, 1988).

Evans, 1988; Evans, 1988). Two of the curves in Fig. 1-1A are from leaves with the same chlorophyll content ($0.48 \text{ mmol Chl m}^{-2}$), but the leaf for the lower curve was grown at 15% of full sunlight. The effect of N content can be separated from the effect of growth irradiance by expressing both axes on the basis of chlorophyll rather than leaf area (Fig. 1-1B). The upper curve represents leaves grown at 100% sunlight and, although their chlorophyll contents differed by a factor of 2.7, the same curve describes them all. The lower two curves represent leaves grown at 30 and 15% of full sunlight. They have the same quantum yield but lower electron-transport capacities per unit of chlorophyll.

The values for J_{max} calculated from gas-exchange characteristics have been compared with the corresponding in vitro uncoupled, light-saturated electron-transport activities for leaves of common bean (*Phaseolus vulgaris* L.) (von Caemmerer & Farquhar, 1981) and spinach (*Spinacia oleracea* L.) (Evans & Terashima, 1988). Variation in J_{max} was obtained by varying the N nutrition or irradiance during growth. In both species, good correlations were found, although the in vitro electron-transport activities were too small to account for the calculated J_{max} . This may simply reflect the incomplete extraction of leaves, damage to the thylakoids, or suboptimal assay conditions. It is frequently observed that Rubisco activity is also barely sufficient to account for the observed rates of CO_2 assimilation by leaves. As discussed below (Fig. 1-2A), the electron-transport and Rubisco capacities co-vary such that, for leaves at high irradiance and at ambient $p\text{CO}_2$, electron-transport and Rubisco capacities co-limit the rate of CO_2 assimilation.